BJ www.biochemj.org

Biochem. J. (2011) **436**, 231–239 (Printed in Great Britain) doi:10.1042/BJ20110083

InsP_3 receptors and Orai channels in pancreatic acinar cells: co-localization and its consequences

Gyorgy LUR*, Mark W. SHERWOOD†, Etsuko EBISUI†, Lee HAYNES*, Stefan FESKE‡, Robert SUTTON§, Robert D. BURGOYNE*, Katsuhiko MIKOSHIBA†, Ole H. PETERSEN‖ and Alexei V. TEPIKIN*[1]

*Department of Cellular and Molecular Physiology, The University of Liverpool, Crown Street, Liverpool L69 3BX, U.K., †Laboratory for Developmental Neurobiology, RIKEN Brain Science Institute, 2-1 Hirosawa, Wako City, Saitama, 351-0198 Japan, ‡NYU Langone Medical Center, 550 First Avenue, SRB 316, New York, NY 10016, U.S.A., §Liverpool NIHR Pancreas Biomedical Research Unit, The University of Liverpool, Crown Street, Liverpool L69 3BX, U.K., and ‖MRC Group, School of Biosciences, Cardiff University, Museum Avenue, Cardiff CF10 3AX, Wales, U.K.

Orai1 proteins have been recently identified as subunits of SOCE (store-operated Ca^{2+} entry) channels. In primary isolated PACs (pancreatic acinar cells), Orai1 showed remarkable co-localization and co-immunoprecipitation with all three subtypes of IP_3Rs (InsP_3 receptors). The co-localization between Orai1 and IP_3Rs was restricted to the apical part of PACs. Neither co-localization nor co-immunoprecipitation was affected by Ca^{2+} store depletion. Importantly we also characterized Orai1 in basal and lateral membranes of PACs. The basal and lateral membranes of PACs have been shown previously to accumulate STIM1 (stromal interaction molecule 1) puncta as a result of Ca^{2+} store depletion. We therefore conclude that these polarized secretory cells contain two pools of Orai1: an apical pool that interacts with IP_3Rs and a basolateral pool that interacts with STIM1 following the Ca^{2+} store depletion. Experiments on IP_3R knockout animals demonstrated that the apical Orai1 localization does not require IP_3Rs and that IP_3Rs are not necessary for the activation of SOCE. However, the InsP_3-releasing secretagogue ACh (acetylcholine) produced a negative modulatory effect on SOCE, suggesting that activated IP_3Rs could have an inhibitory effect on this Ca^{2+} entry mechanism.

Key words: acetylcholine (ACh), Ca^{2+} signalling, InsP_3 receptor (IP_3R), Orai1, pancreatic acinar cell (PAC), store-operated Ca^{2+} entry (SOCE).

INTRODUCTION

PACs (pancreatic acinar cells) are structurally and functionally polarized with secretory granules located in the apical region, whereas the basal and lateral parts contain well-developed rough ER (endoplasmic reticulum). Thin projections of ER are also present in the apical region [1]. Important secretagogues such as ACh (acetylcholine) and CCK (cholecystokinin) utilize InsP_3 and Ca^{2+} signalling cascades to regulate secretion in these cells [2]. The substantial Ca^{2+} extrusion by the PMCAs (plasma membrane Ca^{2+}-ATPases) in PACs [3] necessitates a well-developed SOCE (store-operated Ca^{2+} entry) mechanism. IP_3R2 (InsP_3 receptor 2) and IP_3R3 were shown to be the functional IP_3Rs in PACs [4]. Local apical Ca^{2+} transients can be triggered by InsP_3 [5,6]. All three types of IP_3Rs are found in the apical part of the cell [7–9]. The role of IP_3Rs in the activation of SOCE has been the subject of much debate [10]. The original conformational coupling hypothesis suggested that IP_3Rs in the store activate Ca^{2+} entry channels [11,12]. It was later found that STIM (stromal interaction molecule) proteins serve as the Ca^{2+} sensors in the store; the depletion of ER Ca^{2+} results in the translocation of STIM to the plasma membrane, where it interacts with and activates Orai channels [13–16]. The notion of conformational coupling was therefore confirmed, however, with STIM rather than IP_3R as the primary ER Ca^{2+} sensor. This does not exclude the possibility that IP_3Rs could play some regulatory role in SOCE, particularly considering a recent report describing an interaction between IP_3Rs and Orai1 [17]. In PACs, STIM1 was found to form puncta in the basal and lateral subplasmalemmal regions, where it was also shown to co-localize with Orai1 [18]. The basolateral SOCE in PACs is therefore mediated by STIM1 interacting with Orai1. Surprisingly, the highest density of Orai1 was found in the apical region, away from its activator STIM1 [18], but in the area populated with IP_3Rs [7–9]. This surprising finding led us to examine the relative positioning of the two proteins, which were found to be closely co-localized. In the second part of the present study, we probed the functional consequences of this co-localization.

MATERIALS AND METHODS

Chemicals

All salts as well as ACh, goat serum, BSA and PBS were obtained from Sigma. Collagenase was from Worthington Biochemicals (Lorne Laboratories). TG (thapsigargin) and caffeine were from Calbiochem. Protease inhibitor cocktail was from Roche Diagnostics. Protein G–Sepharose beads were from GE Healthcare. Clean Blot reagent was from Pierce. Fura 2/AM (fura 2 acetoxymethyl ester) and Fluo-4/AM (Fluo-4 acetoxymethyl ester) were from Invitrogen.

Animals and cell isolation

All animal experiments were conducted in accordance with the Animals (Scientific Procedure) Act of 1986. PACs were isolated from the pancreata of CD1 or BL6 [wild-type or specified KO (knockout)] mice using collagenase digestion as described previously [3].

Abbreviations used: ACh, acetylcholine; $[Ca^{2+}]c$, cytosolic Ca^{2+} concentration; ER, endoplasmic reticulum; Fluo-4/AM, Fluo-4 acetoxymethyl ester; fura 2/AM, fura 2 acetoxymethyl ester; IP, immunoprecipitation; IP_3R, InsP_3 receptor; KO, knockout; PAC, pancreatic acinar cell; PMCA, plasma membrane Ca^{2+}-ATPase; SOCE, store-operated Ca^{2+} entry; STIM, stromal interaction molecule; TG, thapsigargin; ZO1, zonula occludens 1.

[1] To whom correspondence should be addressed (email a.tepikin@liv.ac.uk).

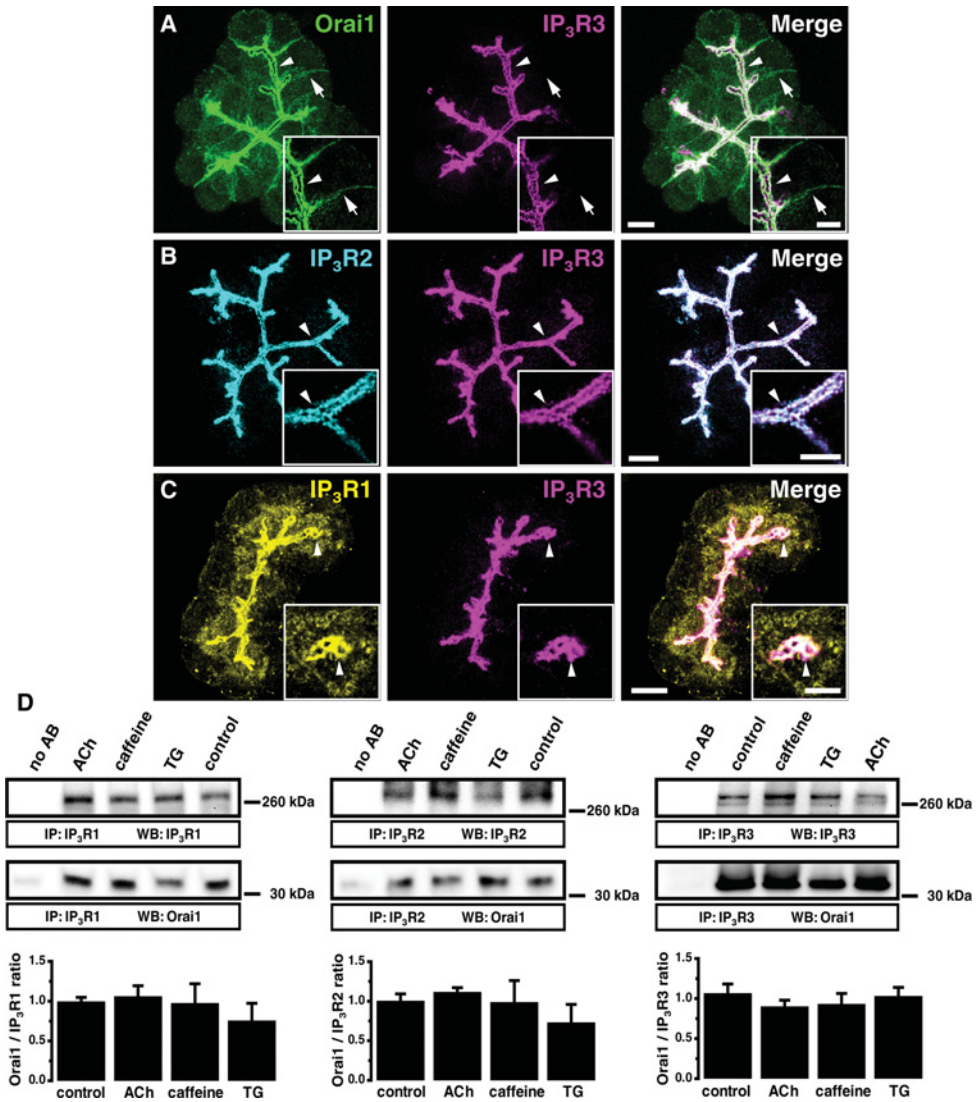

Figure 1 Orai1 co-localization and co-immunoprecipitation with IP_3Rs in PACs

(**A**) Maximum projection of 20 optical sections spaced 1 μm from each other in a PAC cluster. Orai1 (green) is present in both the basolateral (arrows) and apical (arrowheads) regions. In the apical pole, Orai1 co-localizes with IP_3R3 (magenta). Insets: single confocal sections from the same cluster at higher magnification (the arrow and arrowhead points to the same structures as in the main Figure). Here and in (**B**) and (**C**) the scale bars correspond to 10 μm in the projections and 5 μm in the insets. (**B**) Maximum projection of optical sections of a PAC cluster. IP_3R2 (cyan) co-localizes with IP_3R3 (magenta) in the apical pole of the cells (arrowhead). Insets: single confocal sections from the same cluster at higher magnification (the arrowhead points to the same structures as in the main Figure). (**C**) Maximum projection of optical sections of a PAC cluster. The highest density of IP_3R1 (yellow) is observed in the apical pole of the cells (arrowheads), where it co-localizes with IP_3R3 (magenta). Insets: single confocal sections from the same cluster at higher magnification (the arrowhead points to the same structures as in the main Figure). Note that a significant staining for IP_3R1 (unlike that for IP_3R2 and IP_3R3) was also found outside the apical region of the cell. (**D**) Co-immunoprecipitation of Orai1 with IP_3R1 (left panel), IP_3R2 (middle panel) or with IP_3R3 (right panel) in PAC lysates. The first lane in both panels corresponds to beads that were not bound to anti-IP_3R antibodies. Western blots show the IP_3Rs and Orai1 eluted from Sepharose beads decorated with the corresponding IP_3Rs. Histograms show the quantification of Western blots.

Immunofluorescence

Freshly isolated PACs were fixed in methanol for 10 min at − 20 °C. Non-specific antibody binding was blocked for 1 h in 10 % goat serum and 1 % BSA prior to incubation with primary antibodies for 1 h at room temperature (18–21°C). IP_3Rs were visualized by anti-IP_3R3 antibodies (BD Transduction Laboratories) or anti-IP_3R2 antibodies (rabbit polyclonal, raised against the C-terminal amino acids 2686–2702; a gift from Professor D. Yule, School of Medicine and Dentistry, University of Rochester, Rochester, NY, U.S.A.) or anti-IP_3R1 antibodies (rabbit polyclonal, raised against C-terminal amino acids 2735–2749 of mouse IP_3R1; a gift from Professor J. Parys (Laboratory of Molecular and Cellular Signalling, Department of Molecular and Cellular Biology, Catholic University of Leuven, Leuven, Belgium). Orai1 channels were stained with an anti-Orai1 antibody (rabbit polyclonal, raised against C-terminal amino acids 278–294, produced by Dr S. Feske) and tight junctions were visualized by anti-occludin antibodies (Zymed Laboratories, Invitrogen) or anti-ZO1 (zonula occludens 1) antibodies (a gift from Dr M. Furuse, Graduate School of Medicine, Kobe University, Kobe, Japan). Appropriate secondary antibodies conjugated to Alexa Fluor® 488, Alexa Fluor® 594 and/or Alexa Fluor® 647 (Invitrogen) were applied for 30 min and coverslips were mounted on to microscope slides with Prolong Gold (Invitrogen). All fluorescent secondary antibodies, used in the

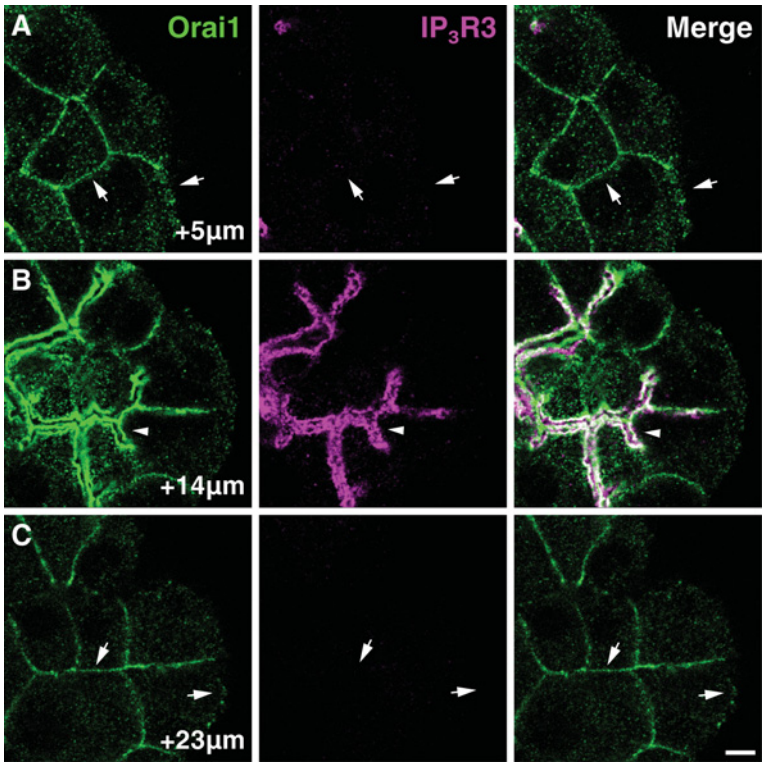

Figure 2 Orai1 only co-localizes with IP_3Rs in the apical region of the acinar cells: apical and basolateral Orai1

(**A**) Confocal section from a cluster of PACs recorded 5 μm from the coverslip. This section is below the apical regions of the cells and Orai1 (green) is clearly visible in the basal and lateral membranes (arrows). (**B**) Confocal section from the same cluster as in (**A**), but recorded 14 μm from the top of the coverslip where IP_3R3s (magenta) decorate the apical surfaces of the cells. Apical Orai1 present in this section (arrowhead) co-localizes with the IP_3R3s. (**C**) Confocal section of the same acinar cell cluster as in (**A**) and (**B**). Confocal section was positioned 23 μm from the coverslip. IP_3Rs are no longer visible as this section is above the apical regions of the cells; however, Orai1 is still present in the lateral and basal membranes (arrows). Scale bars correspond to 5 μm.

present study, were tested on PACs fixed using the same method, but without the application of a primary antibody. None of these secondary antibodies produced any non-specific staining in PACs. Cells were viewed on a Leica TCS SP2 AOBS inverted confocal microscope (Leica Microsystems) equipped with a ×63 oil-immersion objective (numerical aperture = 1.4). Optical sections were spaced by 0.5–1 μm. Linear adjustments of contrast and brightness were applied if necessary in Leica Application Suite.

Ca^{2+} imaging

Freshly isolated PACs were loaded with 2.5 μM fura 2/AM or 2.5 μM Fluo-4/AM for 30 min at room temperature. Fluo-4 labelling was used for experiments involving caffeine. Standard sodium Hepes-based extracellular solution contained 140 mM NaCl, 4.7 mM KCl, 10 mM Hepes, 1 mM $MgCl_2$, 10 mM glucose and 1 mM $CaCl_2$ (pH 7.4). In specific experiments, the Ca^{2+} concentration in this solution was modified (i.e. reduced to nominally Ca^{2+} free or increased to 2 mM). For fura 2 imaging, we utilized Till Photonics Imaging System or a RIKEN BSI Olympus Collaboration Center Imaging System. Fura 2 fluorescence was measured with λ_{ex} at 340 and 380 nm, and λ_{em} using a 510 nm high pass filter. Experiments with Fluo-4 loaded cells were conducted on the Till Photonics Imaging System. Fluo-4 labelling was used for experiments involving caffeine because of the strong effect of caffeine on the fluorescence of fura 2. Fluo-4 fluorescence was measured with λ_{ex} at 470 nm and λ_{em} using a 510 nm high pass filter.

Co-immunoprecipitation and Western blotting

PACs were lysed in IP (immunoprecipitation) buffer containing 50 mM Tris/HCl, 150 mM NaCl, 1 % Triton X-100, 0.25 % sodium deoxycholate, 0.2 % SDS, 2 mM EDTA and 2 × protease inhibitor cocktail. In each condition, lysate containing 600 μg of protein was added to 2 μg of anti-IP_3R antibody (described above) and mixed with 20 μl of Protein G–Sepharose beads in a total volume of 1 ml of IP buffer for 2 h at 4 °C. Proteins were eluted, separated on a 4–12 % Tris/glycine gradient gel and transferred on to nitrocellulose membranes (VWR). Following blocking in 5 % (w/v) non-fat dried skimmed milk powder for 1 h, membranes were probed with anti-Orai1 antibodies (Alomone Labs) and anti-IP_3R antibodies or anti-actin antibodies (Sigma). Following staining with Clean Blot, bands were visualized using ECL (enhanced chemiluminescence) Western-blotting substrate in a Bio-Rad gel documentation system. Bands were quantified using the ImageJ gel quantification plug-in.

RESULTS

Orai1 co-localizes with IP_3Rs in the apical pole of PACs

In the apical pole of PACs, we found a striking co-localization of endogenous Orai1 and IP_3R3 (Figure 1A, $n = 7$). IP_3R2 and IP_3R3 are also co-localized in this cellular region (Figure 1B, $n = 6$). The highest density of IP_3R1 was observed in the apical region where it co-localized with IP_3R3 (Figure 1C, $n = 6$). We can therefore conclude that Orai1 closely co-localizes with all types of IP_3Rs in

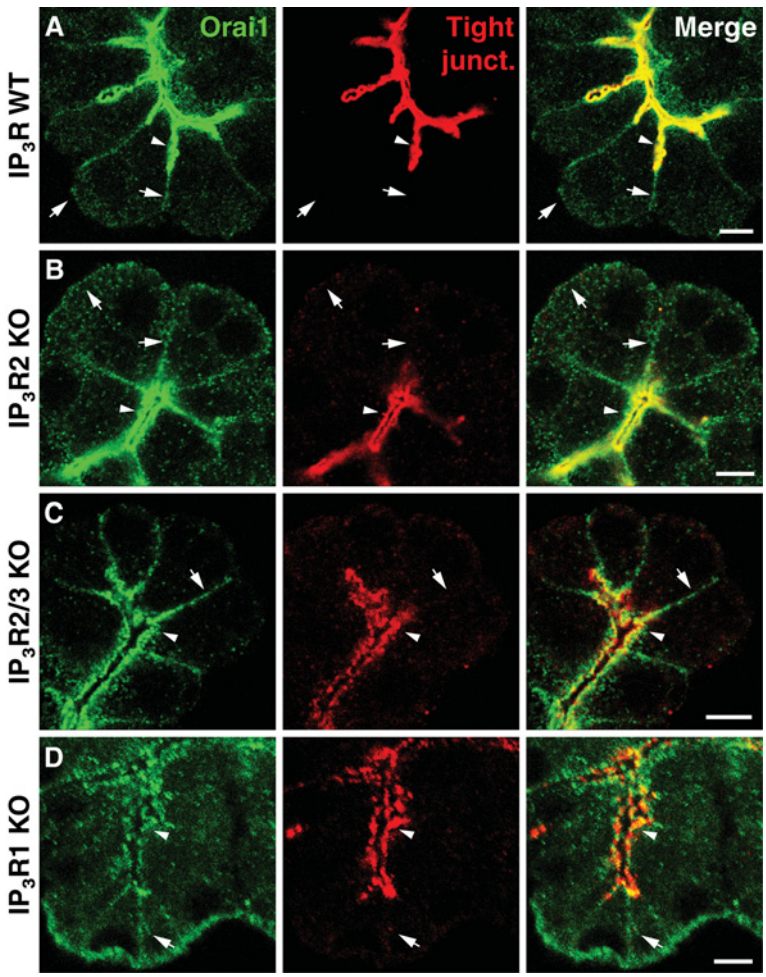

Figure 3 Orai1 is present in the apical pole of acinar cells lacking IP_3Rs

(**A**) Confocal section of an acinar cell cluster isolated from wild-type mouse. Orai1 (green) is visible in basolateral membranes (arrows) and in the apical pole (arrowheads) where it co-localizes with tight junctions (red) marking the apical membrane. (**B**) Confocal section of a cluster of acinar cells isolated from IP_3R2 KO mice. Orai1 is apparent in both apical (arrowhead) and basolateral membranes (arrows), its distribution is similar to that in the cells from wild-type animals. (**C**) Confocal section of an acinar cell cluster isolated from mice lacking both IP_3R2 and IP_3R3 ($IP_3R2/3$ KO). Orai1 is present in basolateral membranes (arrow) as well as in the apical pole (arrowhead) where it co-localizes with tight junction markers. (**D**) Confocal section of an acinar cell cluster isolated from IP_3R1 KO mice. Orai1 staining is visible in the apical pole (arrowhead) and in basolateral membranes (arrow). Scale bars represent 5 μm.

the apical pole of PACs. The apical localization of Orai1 and its co-localization with IP_3R3 did not change in conditions when the cells were treated with the InsP_3-generating secretagogue ACh (Supplementary Figure S1A available at http://www.BiochemJ.org/bj/436/bj4360231add.htm, $n=3$), the IP_3R inhibitor caffeine (Supplementary Figure S1B, $n=3$), or the SERCA (sarcoplasmic/endoplasmic reticulum Ca^{2+}-ATPase) pump inhibitor TG (Supplementary Figure S1C, $n=3$). Orai1 co-immunoprecipitated with all types of IP_3Rs (Figure 1D, $n=6$ for Orai1 and IP_3R1; $n=7$ for Orai1 and IP_3R2; $n=16$ for Orai1 and IP_3R3). This co-immunoprecipitation also did not change significantly when the cells were treated with ACh (Figure 1D, $n=6$ for Orai1 and IP_3R1; $n=7$ for Orai1 and IP_3R2; $n=14$ for Orai1 and IP_3R3), caffeine (Figure 1D, $n=3$ for Orai1 and IP_3R1; $n=5$ for Orai1 and IP_3R2; $n=4$ for Orai1 and IP_3R3) or TG (Figure 1D, $n=3$ for Orai1 and IP_3R1; $n=5$ for Orai1 and IP_3R2; $n=4$ for Orai1 and IP_3R3). Importantly actin (which is present at high density in the apical region) was not co-immunoprecipitated with IP_3Rs (Supplementary Figure S2 available at http://www.BiochemJ.org/bj/436/bj4360231add.htm, $n=4$). The observed co-immunoprecipitation of Orai1 and IP_3Rs does not, of course, guarantee that there is a direct interaction between these proteins, but it is unlikely that the co-immunoprecipitation is due to the interaction of the proteins with actin.

It is essential to note that unlike IP_3Rs, Orai1 was observed not only in the apical region, but also on the basal and lateral membranes (shown by arrows in Figure 1A). This was particularly evident in the optical sections that were recorded below (Figure 2A, section at +5 μm) or above (see Figure 2C, section at +23 μm) the apical region of the cells. Orai1 was clearly present outside the apical region, but the intensity of its immunostaining increased substantially in the apical region decorated with IP_3Rs (see Figure 2B, section at +14 μm) and in this region Orai1 was always found in the close vicinity of IP_3Rs (Figures 1 and 2B, section at +14 μm and Supplementary Figure S1).

Orai1 distribution in PACs lacking IP_3Rs

To find out if the IP_3Rs are required for the apical positioning of Orai1, we imaged the distribution of Orai1 in PACs from IP_3R2 KO mice, from $IP_3R2/3$ double KO mice [4] and from IP_3R1

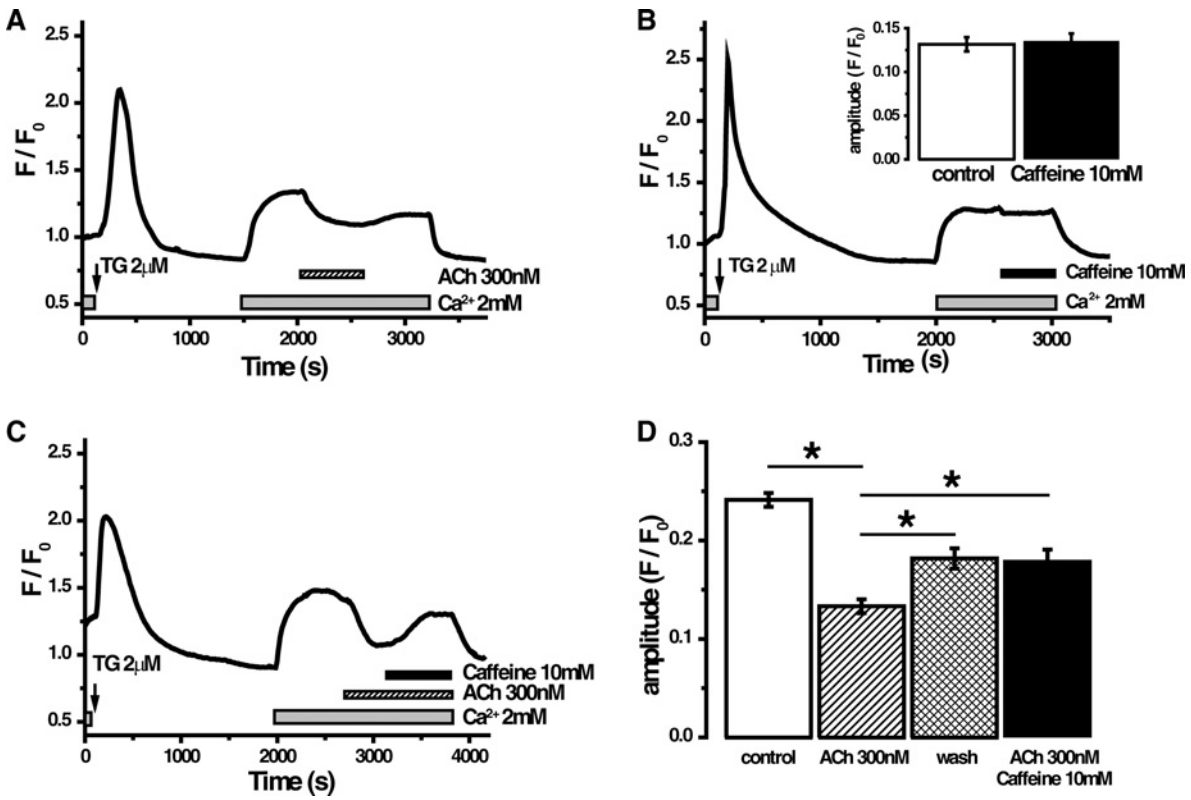

Figure 4 Effect of ACh and caffeine on the cytosolic Ca^{2+} plateau in PACs

(**A**) TG (2 μM)-induced depletion of the ER Ca^{2+} stores in cells placed in the nominally Ca^{2+}-free extracellular solution. Subsequent addition of 2 mM Ca^{2+} to the extracellular solution resulted in the increase in $[Ca^{2+}]$c. ACh application (following the formation of the plateau) caused a decrease in the level of cytosolic Ca^{2+}. Removal of ACh resulted in partial restoration of the amplitude of $[Ca^{2+}]$c. (**B**) The application of caffeine (10 mM) did not affect the $[Ca^{2+}]$c plateau. Inset: quantification of the amplitude of the $[Ca^{2+}]$c plateau before and after addition of caffeine. (**C**) Caffeine treatment partially reverses the effect of ACh on $[Ca^{2+}]$c plateau. (**D**) Quantification of the results illustrated in (**A**)–(**C**). The amplitude of the $[Ca^{2+}]$c plateau was measured before treatment (white bar), following the addition of ACh (striped bar), following the removal of ACh from the extracellular solution (cross-hatched bar) or following the perfusion with the extracellular solution containing both ACh and caffeine (black bar). $^*P < 0.05$.

KO mice [19] produced in K. Mikoshiba's laboratory. The apical membrane region of PACs is enriched with occludin and ZO1 (Supplementary Figure S3 available at http://www.BiochemJ.org/bj/436/bj4360231add.htm). As the apical pole cannot be visualized using anti-IP_3R antibodies in the cells from the double KO animals, we used tight junction markers, i.e. anti-occludin antibodies and/or anti-ZO1 antibodies, to reveal the apical regions in clusters of acinar cells (both antibodies give very similar staining (Supplementary Figure S3) and were co-localized with IP_3Rs in the cells from the wild-type animals (Supplementary Figure S4 available at http://www.BiochemJ.org/bj/436/bj4360231add.htm). In the wild-type animals, Orai1 was mainly found co-localized with these proteins in the apical region, but was also present in the lateral and basal membranes (Figure 3A and Supplementary Movie S1 available at http://www.BiochemJ.org/bj/436/bj4360231add.htm). The distribution of Orai1 in PACs of KO animals was similar to that observed in cells from the wild-type animals (Figure 3). Prominent apical Orai1 staining was present in cells lacking IP_3R2 or both IP_3R2 and IP_3R3 or IP_3R1 (Figures 3B–3D; $n = 5$ for both IP_3R2 KO mice and for $IP_3R2/3$ double KO mice, $n = 3$ for IP_3R1 KO mice). The basolateral presence of Orai1 was also unchanged in the cells from single and double IP_3Rs KO animals (Figure 3). These experiments suggest that IP_3Rs are not required for the targeting of Orai1 to basolateral or apical membrane regions of PACs.

Effects of the InsP_3-generating secretagogue ACh and the IP_3R inhibitor caffeine on SOCE in PACs from the wild-type and IP_3Rs KO mice

In these experiments, TG was used to deplete Ca^{2+} stores in cells maintained in nominally Ca^{2+}-free extracellular solution. Addition of Ca^{2+} to the extracellular solution resulted in SOCE-mediated increase in $[Ca^{2+}]$c (cytosolic Ca^{2+} concentration) followed by formation of an elevated $[Ca^{2+}]$c plateau (Figure 4). Addition of InsP_3-producing secretagogue ACh reversibly decreased the amplitude of the plateau (Figure 4A, $n = 465$). Using the Mn quench technique [20] we also observed a small (13 ± 2 %) but statistically significant inhibition of the influx by 300 nM ACh (Supplementary Figure S5 available at http://www.BiochemJ.org/bj/436/bj4360231add.htm, $n = 145$ cells in ACh-treated group and $n = 139$ cells in control group). Caffeine (10 mM), which in PACs very efficiently blocks InsP_3-induced Ca^{2+} responses [21] has no effect on its own (Figure 4B, $n = 169$), but it partially reversed the ACh-induced reduction of the plateau (Figure 4C, $n = 168$). These experiments suggest that activation of IP_3Rs has a mild inhibitory rather than stimulatory action on SOCE. Caffeine efficiently quenches fura 2, because of this property the experiments described above were conducted using single wavelength indicator fluo-4. We further tested the effects of ACh on TG-induced $[Ca^{2+}]$c plateau using the ratiometric probe

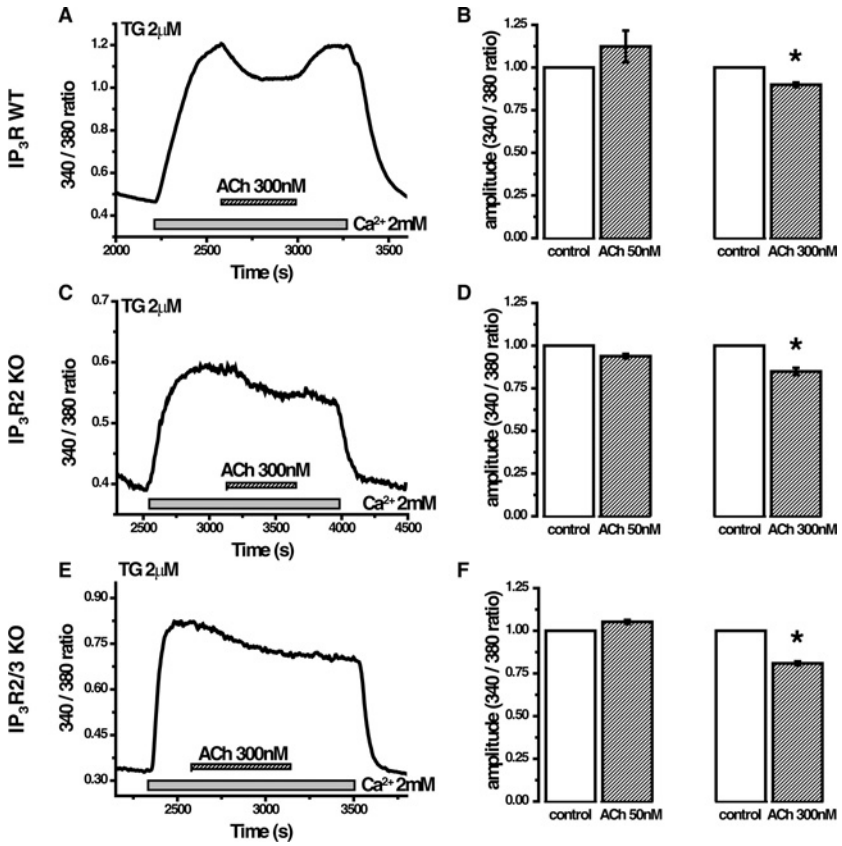

Figure 5 Effect of ACh on the cytosolic Ca^{2+} plateau in acinar cells isolated from wild-type and IP_3R KO mice

(**A**) Intracellular Ca^{2+} stores of fura 2-loaded PACs, isolated from wild-type mice were depleted during a 30 min preincubation in nominally Ca^{2+}-free extracellular solution containing 2 μM TG. The addition of 2 mM Ca^{2+} to the extracellular solution resulted in the formation of a $[Ca^{2+}]$c plateau. Subsequent ACh application triggered a small drop of the plateau that could be reversed by removal of ACh. (**B**) Normalized (to the plateau level before ACh addition) plateau amplitude before (white bars) and following (striped bars) treatment with 50 or 300 nM ACh. Only the application of a large concentration of ACh (300 nM) caused a significant reduction of the plateau amplitude in PACs from wild-type mice (paired Student's *t*-test, $^*P < 0.05$). (**C**) Intracellular Ca^{2+} stores of fura 2-loaded PACs, isolated from IP_3R2 KO mice, were depleted with 2 μM TG in nominally Ca^{2+}-free extracellular solution and subsequent addition of 2 mM Ca^{2+} resulted in the formation of a $[Ca^{2+}]$c plateau. The application of a large concentration of ACh resulted in a small decrease in the plateau. (**D**) Normalized plateau amplitude, recorded from PACs from IP_3R2 KO mice, before (white bars) and following (striped bars) treatment with 50 or 300 nM ACh. Only the application of a 300 nM ACh caused a significant reduction of plateau amplitude in PACs from IP_3R2 KO mice (paired Student's *t*-test, $^*P < 0.05$). (**E**) Intracellular Ca^{2+} stores of fura 2-loaded PACs, isolated from $IP_3R2/3$ KO mice, were depleted as described above and a cytosolic Ca^{2+} plateau was formed by introducing 2 mM Ca^{2+} to the extracellular solution. Subsequent addition of ACh resulted in a decrease in cytosolic Ca^{2+} levels. (**F**) Normalized plateau amplitude, recorded from PACs from $IP_3R2/3$ KO mice before (white bars) and following (striped bars) treatment with 50 or 300 nM ACh. Only the application of a 300 nM ACh caused a small but statistically significant reduction of plateau amplitude (paired Student's *t*-test, $^*P <$ 0.05).

fura 2. The results were similar to that observed using fluo-4, i.e. 300 nM ACh (but not 50 nM ACh) reversibly decreased TG-induced $[Ca^{2+}]$c plateau (Figures 5A and 5B, $n = 61$ for 50 nM ACh and $n = 62$ for 300 nM ACh). Similar results were found in experiments on PACs from IP_3R2 KO mice (Figures 5C and 5D, $n = 47$ for 50 nM ACh and $n = 33$ for 300 nM ACh) and from $IP_3R2/3$ double KO mice (Figures 5E and 5F, $n = 46$ for 50 nM ACh and $n = 31$ for 300 nM ACh); although the recovery phase (on removal of ACh) was less clear in experiments on KO and double KO mice. To assess SOCE more directly and provide an internal control for each experiment we used a two pulse protocol, where cellular Ca^{2+} stores were depleted using TG in nominally Ca^{2+}-free external solution and then two short pulses of extracellular calcium (2 mM) were applied (Figure 6A). The first pulse (after the TG-induced Ca^{2+} store depletion) was applied in agonist-free extracellular medium, whereas the second pulse was applied in the presence of ACh (Figure 6A) or in agonist-free extracellular medium (control, results not shown). The changes in the fura 2 340 nm/380 nm ratio were differentiated (the procedure is illustrated in the inset in Figure 6A) and the maximal rate determined. Considering the relatively slow Ca^{2+} extrusion by PMCA at or near the resting $[Ca^{2+}]$c [3] and taking into account that the maximal rates of changes were also observed at close to resting $[Ca^{2+}]$c, we can assume that the maximal derivative reflects the maximal SOCE rate. The maximal SOCE rate during the second pulse was normalized to that recorded during the first pulse, in order to provide an internal control for every cell in each experiment (Figures 6A and 6B). In wild-type cells, a low concentration of ACh (50 nM) slightly reduced the SOCE rate (by $10 \pm 3\%$, $n = 61$; Figure 6B), whereas the treatment with 300 nM ACh resulted in a reduction in the SOCE rate of $27 \pm 4\%$ ($n = 62$, Figure 6B). In similar experiments (Supplementary Figure S6 available at http://www.BiochemJ.org/bj/436/bj4360231add.htm), we tested the effect of caffeine on SOCE rate. Caffeine (10 mM) alone did not affect SOCE rate (Supplementary Figure S6, $n = 48$). The ability of ACh to inhibit SOCE was further tested using the two-pulse protocol on the PACs from IP_3R2 single KO and $IP_3R2/3$ double KO mice (Figures 6C–6F). These experiments showed that both concentrations of ACh-induced small, but statistically

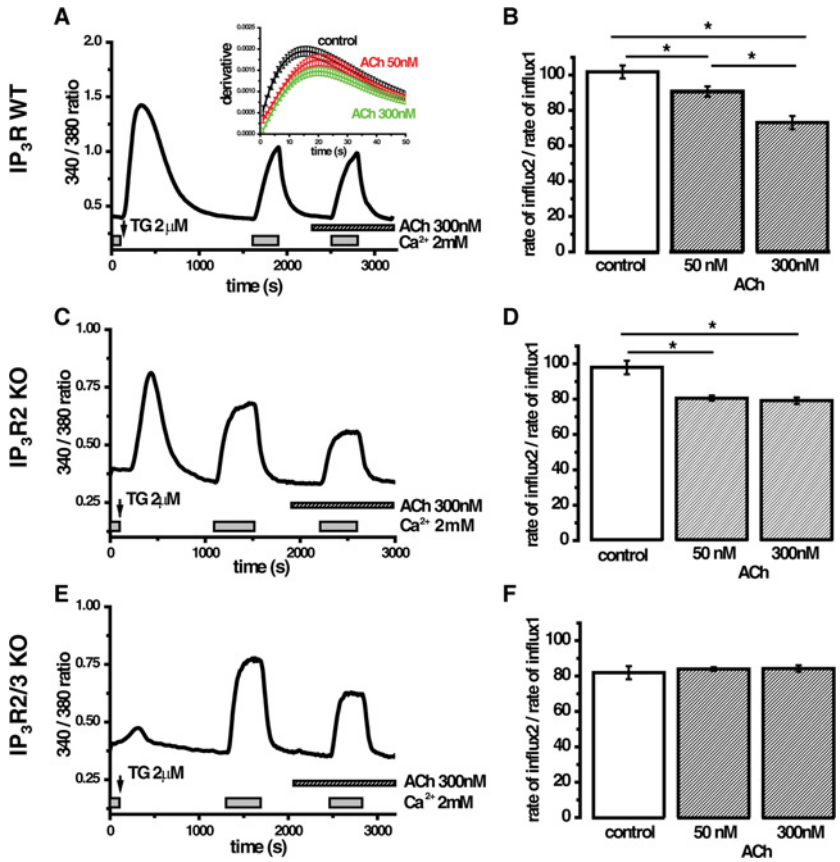

Figure 6 Effects of ACh on the rate of SOCE in PACs isolated from wild-type and IP_3R KO mice

(**A**) Fura 2 ratio changes upon TG treatment and pulses of external Ca^{2+} in the absence and presence of 300 nM ACh in PACs from the wild-type animals. To assess the rate of Ca^{2+} influx the rising phase (induced by a short pulse of 2 mM Ca^{2+}) of the curve was differentiated and the maximum rate of influx was estimated as the maximal value of the derivative (see inset). The same procedure was repeated for the second pulse of external Ca^{2+} (delivered in the presence or absence of ACh). (**B**) Summary of the effects of 50 nM ACh and 300 nM ACh on SOCE rate in the cells from wild-type animals. Here, as well as in (**D**) and (**F**), the statistical significance was probed by ANOVA, $^*P < 0.05$. (**C**) Fura 2 ratio changes upon TG treatment and pulses of external Ca^{2+} in the absence and presence of 300 nM ACh in PACs from IP_3R2 KO mice. (**D**) Summary of the effects of 50 and 300 nM ACh on SOCE rate in the cells from IP_3R2 KO mice. (**E**) Fura 2 ratio changes upon TG treatment and pulses of external Ca^{2+} in the absence and presence of 300 nM ACh in PACs from $IP_3R2/3$ double KO mice. (**F**) Summary graph showing SOCE rate in control conditions and in the presence of 50 or 300 nM ACh in the cells from $IP_3R2/3$ double KO mice.

significant, reductions in the SOCE rate in PACs from IP_3R2 KO mice (Figures 6C and 6D). Both concentrations reduced SOCE rate by 20 ± 2 %. These results were qualitatively similar to those obtained in cells from wild-type animals. The Ca^{2+} responses in cells from the $IP_3R2/3$ double KO mice were different: the response to TG was drastically reduced in comparison with that in the wild-type and the single KO mice (Figure 6E compared with Figures 6A and 6C). This suggests that IP_3Rs amplify the TG response by Ca^{2+}-induced Ca^{2+} release and that this amplification mechanism is absent in $IP_3R2/3$ double KO mice. The responses to the external Ca^{2+} pulses in PACs from the double KO mice were, however, surprisingly robust (Figure 6E). In fact the maximal SOCE rate during the first pulse was slightly higher in the cells from the double KO mice (26 % higher) than the single KO mice. Using the two-pulse protocol we have not observed changes in the SOCE rate upon the application of 50 or 300 nM ACh in the cells from double KO animals (Figure 6F, $n = 67$ for 50 nM and $n = 76$ for 300 nM). The SOCE rate during the second pulse was however already reduced by approx. 20 % in comparison with the first pulse even under control (no ACh) conditions (Figure 6F). It is therefore possible that we do not observe ACh-induced SOCE suppression in these experiments because the ACh simply cannot inhibit the Ca^{2+} influx any further.

DISCUSSION

PACs structurally satisfy the requirements for IP_3R and store-operated Ca^{2+} channel interaction (see Figure 1) suggested as the basis for the original conformational-coupling theory of SOCE [11,12]. We were not able to detect SOCE up-regulation in response to stimulation with the InsP_3-producing agonist ACh. The inhibition of IP_3Rs with caffeine also had no affect on SOCE. In these respects, the present study yielded important negative results. This finding is in line with conclusions from the study by Woodard et al. [17], which highlighted the importance of the interaction between IP_3Rs and Orai1 for different Ca^{2+} signalling processes, but indicated that the disruption of the interaction between IP_3R1 and Orai1 does not prevent TG-induced SOCE and has no significant effect on this process.

The ACh application experiments suggest that IP_3Rs could negatively regulate SOCE. This negative modulation could offer some protection against Ca^{2+} overload induced by InsP_3-producing secretagogues. The effect of ACh is, however, moderate and SOCE develops efficiently in the acinar cells lacking both functional types of IP_3Rs.

In the present study, the highest density of Orai1 was observed in the apical part of the cell containing IP_3Rs, occludin and ZO-1.

Importantly, we also found Orai1 along the lateral and basal membranes, far beyond the region containing tight junctions and IP_3Rs (Figures 1–3 and Supplementary Movie S1). In this basolateral region, Orai1 was shown to co-localize with STIM1 and form Orai1 and STIM1 puncta following ER store depletion [18]. It is possible that two mechanisms of SOCE operate in PACs; basolateral SOCE mediated by STIM1 and Orai1 proteins will have a reliable Ca^{2+} source delivered by the interstitial fluid, whereas apical SOCE could help to re-capture Ca^{2+} transported paracellularly [22], extruded by PMCA (which are active in the apical region [23,24]) and exocytosed with the content of secretory granules. It is conceivable that apical Orai1 could play a role in preventing the build-up of Ca^{2+} in pancreatic ducts, and consequently, pancreatic stone formation in these structures. The close co-positioning of IP_3Rs and Orai1 in the apical region suggests that if activated the apical Orai1 could efficiently re-load strategically important (IP_3R containing) Ca^{2+} stores. The ability of the apical Orai1 to participate in SOCE, the putative mechanism of activation and the physiological function of the apical Orai1 will need to be determined in a separate study. While the present paper was in revision, a study was published by Hong et al. [25] indicating that Orai1 is localized in the apical part of acinar cells where it co-localized with IP_3R3. The important difference between this study and our paper is that we observed a substantial presence of Orai1 in the plasma membrane regions outside the apical pole. Indeed our confocal images (Figure 1, Supplementary Figure S1, Figure 3, Supplementary Movie S1 and particularly Figure 2) clearly reveal substantial Orai1 staining outside the plasma membrane regions decorated with IP_3Rs, occludin or ZO-1. Also contrary to conclusions from Hong et al. [25] (but see Figure 5A in [25]), in our previous work we have not observed apical localization of STIM1 in cells with depleted ER Ca^{2+} stores [18]. We therefore consider that the apical function of Orai1 is likely to be STIM1-independent. It is also important to note that the previous electron microscopy investigation of the sub-plasmalemmal ER and the plasma membrane in PACs, revealed ribosome-free rough ER junctions decorated with STIM1 in basal and lateral sub-plasmalemmal regions, but not in the apical pole of the cell [18]. It is therefore difficult to reconcile some of the conclusions (specifically the role of STIM1 in activating apical Orai1 channels) of Hong et al. [25] and our study.

The present study revealed close positioning of IP_3Rs and Orai1 channels in the apical pole of the PACs, documented the presence of Orai1 in the apical region of the cells lacking functional IP_3Rs and concluded that, in spite of the remarkably close localization of the two proteins, IP_3Rs do not activate SOCE in the apical region of PACs.

AUTHOR CONTRIBUTION

Gyorgy Lur and Mark Sherwood conducted experiments; Gyorgy Lur, Mark Sherwood, Etsuko Ebisui, Lee Haynes, Stefan Feske, Robert Sutton, Robert Burgoyne, Katsuhiko Mikoshiba, Ole Petersen and Alexei Tepikin designed the research project and provided advice on experimental design; and Gyorgy Lur and Alexei Tepikin wrote the paper.

ACKNOWLEDGEMENTS

We acknowledge support from RIKEN BSI-Olympus Collaboration Centre. The authors declare no conflict of interest, except S. F., who is a scientific co-founder of CalciMedica.

FUNDING

This work was supported by the Medical Research Council (U.K.) [grant numbers G0700167, G19/22]; the Wellcome Trust [grant number 080906/Z/06/Z]; and a National Institute for Health Research (U.K.) grant to the Liverpool NIHR Pancreas Biomedical Research Unit. K. M. was supported by a Japan Science and Technology Agency (Japan) grant (Ca^{2+} oscillations project). S. F. was supported by a National Institutes of Health (U.S.A.) grant [grant number AI066128]. M. S. is a RIKEN Foreign Postdoctoral Research Fellow.

REFERENCES

1 Park, M. K., Petersen, O. H. and Tepikin, A. V. (2000) The endoplasmic reticulum as one continuous Ca(2+) pool: visualization of rapid Ca(2+) movements and equilibration. EMBO J. **19**, 5729–5739
2 Petersen, O. H. and Tepikin, A. V. (2008) Polarized calcium signaling in exocrine gland cells. Annu. Rev. Physiol. **70**, 273–299
3 Tepikin, A. V., Voronina, S. G., Gallacher, D. V. and Petersen, O. H. (1992) Pulsatile Ca^{2+} extrusion from single pancreatic acinar cells during receptor-activated cytosolic Ca^{2+} spiking. J. Biol. Chem. **267**, 14073–14076
4 Futatsugi, A., Nakamura, T., Yamada, M. K., Ebisui, E., Nakamura, K., Uchida, K., Kitaguchi, T., Takahashi-Iwanaga, H., Noda, T., Aruga, J. and Mikoshiba, K. (2005) IP_3 receptor types 2 and 3 mediate exocrine secretion underlying energy metabolism. Science **309**, 2232–2234
5 Ito, K., Miyashita, Y. and Kasai, H. (1997) Micromolar and submicromolar Ca^{2+} spikes regulating distinct cellular functions in pancreatic acinar cells. EMBO J. **16**, 242–251
6 Thorn, P., Lawrie, A. M., Smith, P. M., Gallacher, D. V. and Petersen, O. H. (1993) Local and global cytosolic Ca^{2+} oscillations in exocrine cells evoked by agonists and inositol trisphosphate. Cell **74**, 661–668
7 Lee, M. G., Xu, X., Zeng, W., Diaz, J., Wojcikiewicz, R. J., Kuo, T. H., Wuytack, F., Racymaekers, L. and Muallem, S. (1997) Polarized expression of Ca^{2+} channels in pancreatic and salivary gland cells. Correlation with initiation and propagation of $[Ca^{2+}]i$ waves. J. Biol. Chem. **272**, 15765–15770
8 Nathanson, M. H., Fallon, M. B., Padfield, P. J. and Maranto, A. R. (1994) Localization of the type 3 inositol 1,4,5-trisphosphate receptor in the Ca^{2+} wave trigger zone of pancreatic acinar cells. J. Biol. Chem. **269**, 4693–4696
9 Yule, D. I., Ernst, S. A., Ohnishi, H. and Wojcikiewicz, R. J. (1997) Evidence that zymogen granules are not a physiologically relevant calcium pool. Defining the distribution of inositol 1,4,5-trisphosphate receptors in pancreatic acinar cells. J. Biol. Chem. **272**, 9093–9098
10 Parekh, A. B. and Putney, Jr, J. W. (2005) Store-operated calcium channels. Physiol. Rev. **85**, 757–810
11 Berridge, M. J. (1995) Capacitative calcium entry. Biochem. J. **312**, 1–11
12 Irvine, R. F. (1990) 'Quantal' Ca^{2+} release and the control of Ca^{2+} entry by inositol phosphates – a possible mechanism. FEBS Lett. **263**, 5–9
13 Feske, S., Gwack, Y., Prakriya, M., Srikanth, S., Puppel, S. H., Tanasa, B., Hogan, P. G., Lewis, R. S., Daly, M. and Rao, A. (2006) A mutation in Orai1 causes immune deficiency by abrogating CRAC channel function. Nature **441**, 179–185
14 Liou, J., Kim, M. L., Heo, W. D., Jones, J. T., Myers, J. W., Ferrell, Jr, J. E. and Meyer, T. (2005) STIM is a Ca^{2+} sensor essential for Ca^{2+}-store-depletion-triggered Ca^{2+} influx. Curr. Biol. **15**, 1235–1241
15 Luik, R. M., Wu, M. M., Buchanan, J. and Lewis, R. S. (2006) The elementary unit of store-operated Ca^{2+} entry: local activation of CRAC channels by STIM1 at ER-plasma membrane junctions. J. Cell Biol. **174**, 815–825
16 Roos, J., DiGregorio, P. J., Yeromin, A. V., Ohlsen, K., Lioudyno, M., Zhang, S., Safrina, O., Kozak, J. A., Wagner, S. L., Cahalan, M. D. et al. (2005) STIM1, an essential and conserved component of store-operated Ca^{2+} channel function. J. Cell Biol. **169**, 435–445
17 Woodard, G. E., Lopez, J. J., Jardin, I., Salido, G. M. and Rosado, J. A. (2010) TRPC3 regulates agonist-stimulated Ca^{2+} mobilization by mediating the interaction between type I inositol 1,4,5-trisphosphate receptor, RACK1, and Orai1. J. Biol. Chem. **285**, 8045–8053
18 Lur, G., Haynes, L. P., Prior, I. A., Gerasimenko, O. V., Feske, S., Petersen, O. H., Burgoyne, R. D. and Tepikin, A. V. (2009) Ribosome-free terminals of rough ER allow formation of STIM1 puncta and segregation of STIM1 from IP(3) receptors. Curr. Biol. **19**, 1648–1653
19 Matsumoto, M., Nakagawa, T., Inoue, T., Nagata, E., Tanaka, K., Takano, H., Minowa, O., Kuno, J., Sakakibara, S., Yamada, M. et al. (1996) Ataxia and epileptic seizures in mice lacking type 1 inositol 1,4,5-trisphosphate receptor. Nature **379**, 168–171
20 Barrow, S. L., Voronina, S. G., da, S., X, Chvanov, M. A., Longbottom, R. E., Gerasimenko, O. V., Petersen, O. H., Rutter, G. A. and Tepikin, A. V. (2008) ATP depletion inhibits Ca^{2+} release, influx and extrusion in pancreatic acinar cells but not pathological Ca^{2+} responses induced by bile. Pflugers Arch. **455**, 1025–1039
21 Toescu, E. C., O'Neill, S. C., Petersen, O. H. and Eisner, D. A. (1992) Caffeine inhibits the agonist-evoked cytosolic Ca^{2+} signal in mouse pancreatic acinar cells by blocking inositol trisphosphate production. J. Biol. Chem. **267**, 23467–23470

22 Jansen, J. W., Schreurs, V. V., Swarts, H. G., Fleuren-Jakobs, A. M., de Pont, J. J. and Bonting, S. L. (1980) Role of calcium in exocrine pancreatic secreation. VI. Characteristics of the paracellular pathway for divalent cations. Biochim. Biophys. Acta **599**, 315–323

23 Belan, P. V., Gerasimenko, O. V., Tepikin, A. V. and Petersen, O. H. (1996) Localization of Ca^{2+} extrusion sites in pancreatic acinar cells. J. Biol. Chem. **271**, 7615–7619

24 Lee, M. G., Xu, X., Zeng, W., Diaz, J., Kuo, T. H., Wuytack, F., Racymaekers, L. and Muallem, S. (1997) Polarized expression of Ca^{2+} pumps in pancreatic and salivary gland cells. Role in initiation and propagation of $[Ca^{2+}]i$ waves. J. Biol. Chem. **272**, 15771–15776

25 Hong, J. H., Li, Q., Kim, M. S., Shin, D. M., Feske, S., Birnbaumer, L., Cheng, K. T., Ambudkar, I. S. and Muallem, S. (2011) Polarized but differential localization and recruitment of STIM1, Orai1 and TRPC channels in secretory cells. Traffic **12**, 232–245

Received 13 January 2011/1 March 2011; accepted 3 March 2011
Published as BJ Immediate Publication 3 March 2011, doi:10.1042/BJ20110083

Biochem. J. (2011) **436**, 231–239 (Printed in Great Britain) doi:10.1042/BJ20110083

multimedia online data

SUPPLEMENTARY ONLINE DATA

InsP_3 receptors and Orai channels in pancreatic acinar cells: co-localization and its consequences

Gyorgy LUR*, Mark W. SHERWOOD†, Etsuko EBISUI†, Lee HAYNES*, Stefan FESKE‡, Robert SUTTON§, Robert D. BURGOYNE*, Katsuhiko MIKOSHIBA†, Ole H. PETERSEN‖ and Alexei V. TEPIKIN*[1]

*Department of Cellular and Molecular Physiology, The University of Liverpool, Crown Street, Liverpool L69 3BX, U.K., †Laboratory for Developmental Neurobiology, RIKEN Brain Science Institute, 2-1 Hirosawa, Wako City, Saitama, 351-0198 Japan, ‡NYU Langone Medical Center, 550 First Avenue, SRB 316, New York, NY 10016, U.S.A., §Liverpool NIHR Pancreas Biomedical Research Unit, The University of Liverpool, Crown Street, Liverpool L69 3BX, U.K., and ‖MRC Group, School of Biosciences, Cardiff University, Museum Avenue, Cardiff CF10 3AX, Wales, U.K.

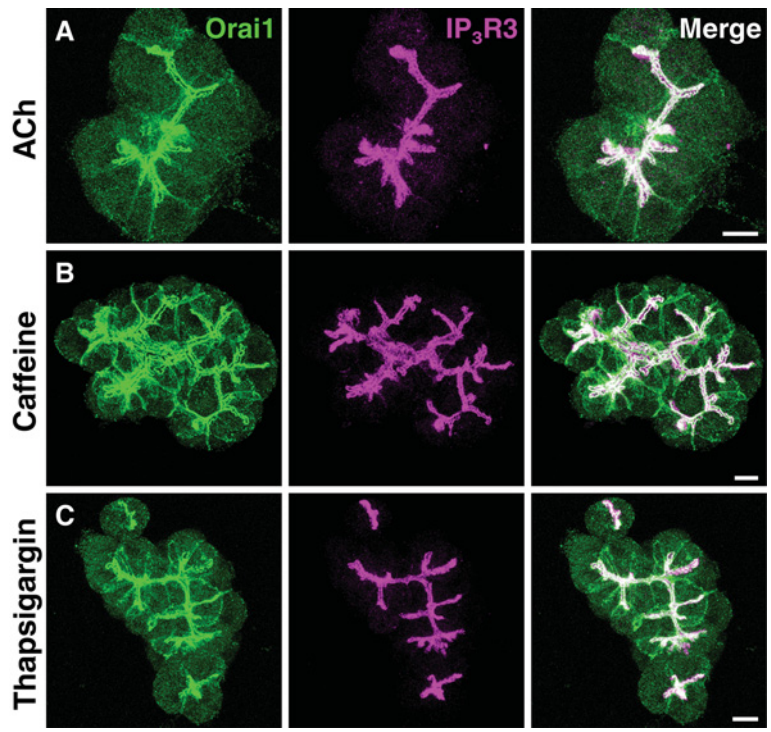

Figure S1 Orai1 and IP_3R3 staining in acinar cells following various stimuli

All images show maximum projections of confocal optical slices from pancreatic acinar cell clusters. The distribution of Orai1 (green) in pancreatic acinar cells in the presence of (**A**) ACh (300 nM, $n = 3$), (**B**) caffeine (10 mM, $n = 3$) and (**C**) TG (2 μM, $n = 3$). In the apical pole, Orai1 was co-localized with type 3 IP_3Rs (magenta) in every condition. Note that we have not observed clearance of Orai1 or IP_3R3 from the apical region following the ACh stimulation, which should trigger significant exocytosis of zymogen granules and therefore additional membrane turnover in the apical region of the cells. The distribution of Orai1 and IP_3R3 was similar to that in control (unstimulated) cells. Some lateral and basal Orai was observed (**A**–**C** right panels, green colour on the merged images). Scale bars correspond to 10 μm.

[1] To whom correspondence should be addressed (email a.tepikin@liv.ac.uk).

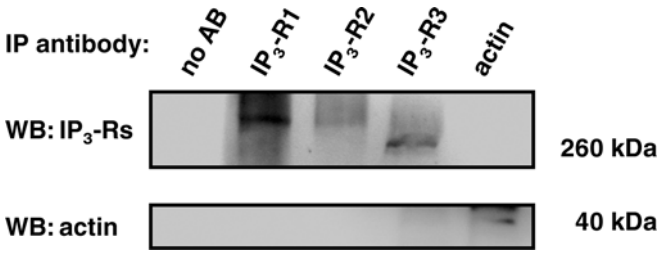

Figure S2 IP_3Rs do not co-immunoprecipitate actin from pancreatic acinar cells

Western blots show immunoprecipitates from pancreatic acinar cell lysates. Protein G–Sepharose beads without antibodies (no AB) do not precipitate significant amounts of protein from acinar cell lysates (lane 1). Antibodies against all three subtypes of IP_3Rs precipitate the corresponding IP_3R (lanes 2–4, upper panel) but not actin (same lanes on the lower panel), while an anti-actin antibody precipitates actin from the lysate but none of the three IP_3Rs (lane 5). Hence it is unlikely that the observed IP_3R–Orai1 co-immunoprecipitation (reported in the main paper and illustrated in Figure 1 of the main paper) is mediated by actin.

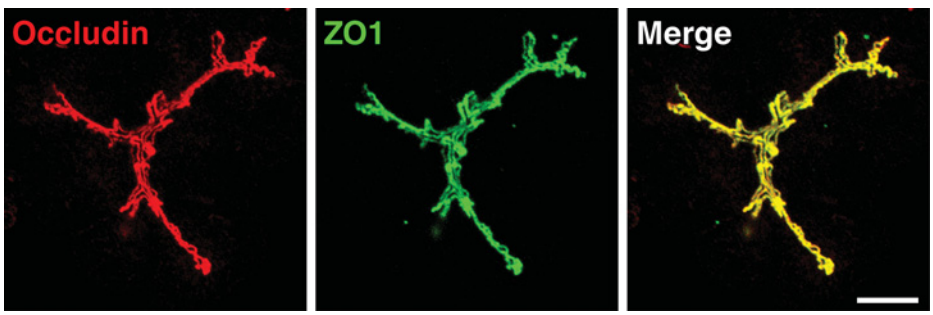

Figure S3 Occludin and ZO1 co-localize in pancreatic acinar cells

Antibodies against occludin or ZO1 were used (see Figure 3 and accompanying text in the main paper) to probe the localization of tight junctions and to define the apical membrane regions of the cells. Anti-ZO1 antibody [1] was a gift from Dr M. Furuse from Kobe University. The images demonstrate the co-localization of the two proteins ($n = 4$) which both can therefore be used to label tight junctions. Scale bar corresponds to 10 μm.

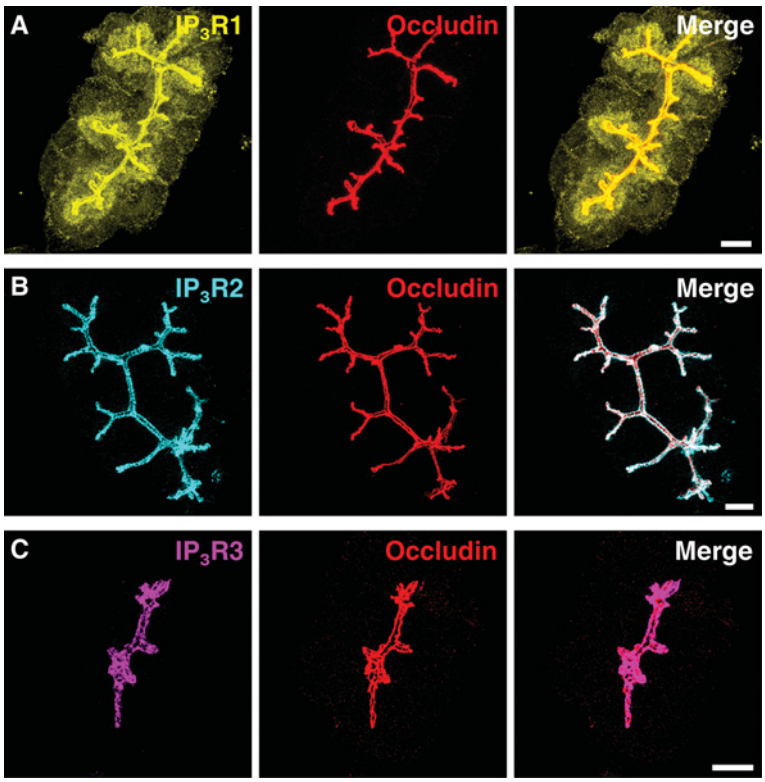

Figure S4 Apically localized IP_3Rs co-localize with tight junction marker occludin

Images show the maximum projections of optical sections from pancreatic acinar cell clusters. IP_3R1 (yellow, **A**), IP_3R2 (cyan, **B**) and IP_3R3 (magenta, **C**) co-localize with occludin (red, central panels) in the apex of acinar cells ($n = 3$, 4 and 3 respectively). Merged images are shown in the right-hand panels. Scale bars correspond to 10 μm.

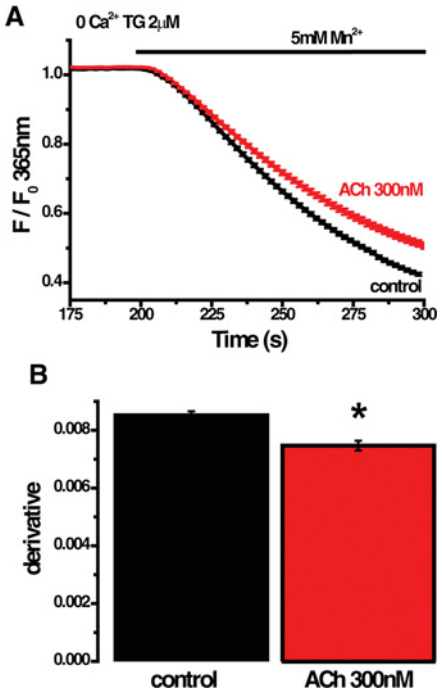

Figure S5 Effect of ACh on Mn^{2+} influx in pancreatic ainar cells

(**A**) Intracellular Ca^{2+} stores of fura 2-loaded acinar cells were depleted by a 15 min pre-incubation with nominally Ca^{2+}-free extracellular solution containing 2 μM TG . To assess the effect of ACh on Mn^{2+} entry, store-depleted cells were treated for an additional 5 min with Ca^{2+}-free extracellular solution containing 2 μM TG (control, black trace, $n = 139$) or 2 μM TG and 300 nM ACh (red trace, $n = 145$). Subsequently 5 mM Mn^{2+} was added to the solutions. (**A**) Shows average traces $\pm$S.E.M. (**B**) Quantification (averaged maximal amplitude of the derivatives of individual traces) of Mn^{2+} quench in control (black bar) and in ACh (300 nM, red bar)-treated acinar cells. The rate of fura 2 quench was measured by differentiating the declining part (caused by the addition of 5 mM Mn^{2+}) of the curve and determining the maximal amplitude of the derivative.

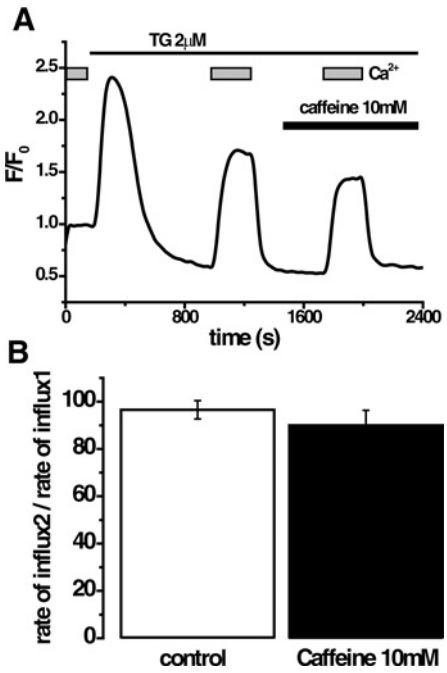

Figure S6 Inhibition of IP_3Rs by caffeine does not affect the rate of SOCE in acinar cells

Fluo-4 was used as the cytosolic Ca^{2+} indicator in experiments involving caffeine because of the strong effect of caffeine on fluorescence of fura 2 [2]. Caffeine was shown to efficiently inhibit InsP_3-induced Ca^{2+} responses in pancreatic acinar cells [3] as well as responses to InsP_3-producing secretagogues [2]. (**A**) Example trace illustrates an experiment designed to test the effect of caffeine using the double pulse protocol (for details of the procedure see Figure 6 and the accompanying text in the main paper). Acinar cells were placed in nominally Ca^{2+}-free extracellular solution and internal Ca^{2+} stores were depleted by the addition of 2 μM TG to the bath. Following store depletion two calcium pulses (2 mM) were applied to measure the effect of caffeine on store operated Ca^{2+} entry. The curves were differentiated and the maximal derivative attained during external Ca^{2+} pulses determined. (**B**) SOCE rate (averaged and normalized maximal derivative) in control conditions (white bar) and in the presence of caffeine (black bar). Caffeine had no statistically significant effect on the maximal SOCE rate (probed using Student's *t*-test).

REFERENCES

1 Itoh, M., Yonemura, S., Nagafuchi, A., Tsukita, S. and Tsukita, S. (1991) A 220-kD undercoat-constitutive protein: its specific localization at cadherin-based cell-cell adhesion sites. J. Cell Biol. **115**, 1449–1462

2 Toescu, E. C., O'Neill, S. C., Petersen, O. H. and Eisner, D. A. (1992) Caffeine inhibits the agonist-evoked cytosolic Ca^{2+} signal in mouse pancreatic acinar cells by blocking inositol trisphosphate production. J. Biol. Chem. **267**, 23467–23470

3 Wakui, M., Osipchuk, Y. V. and Petersen, O. H. (1990) Receptor-activated cytoplasmic Ca^{2+} spiking mediated by inositol trisphosphate is due to Ca^{2+}-induced Ca^{2+} release. Cell **63**, 1025–1032

Received 13 January 2011/1 March 2011; accepted 3 March 2011
Published as BJ Immediate Publication 3 March 2011, doi:10.1042/BJ20110083